Partially Fluorinated Thioethers at the Water/Air Interface. Langmuir Monolayer Characterization and X-ray Scattering Studies

Marcin Broniatowski,*,† Michał Flasiński,† Patrycja Dynarowicz-Łatka,† and Jarosław Majewski‡

Faculty of Chemistry, Jagiellonian University, Ingardena 3, 30-060 Kraków, Poland, and Lujan Neutron Scattering Center, Los Alamos National Laboratory, Los Alamos, New Mexico 87545

Received: June 3, 2010; Revised Manuscript Received: August 29, 2010

A series of partially fluorinated aliphatic thioethers of the following formula: $CF_3-(CF_2)_7-(CH_2)_{10}-S-C_nH_{2n+1}$, where $n = 1$, 2, 4, 8, 12, and 18, were synthesized and spread from chloroform solution onto the water/air interface in a Langmuir trough. Upon compression of the film, the surface pressure−mean molecular area isotherms were recorded. It turned out that all the investigated compounds are capable of stable Langmuir monolayers formation. The electrical properties of the studied monolayers have been investigated by monitoring the change in the surface potential (ΔV) upon film compression. The performed experiments proved that regardless of the length of the C_nH_{2n+1} chain, the orientation of the film molecules is very similar. The investigated monolayers have been visualized applying Brewster angle microscopy. The monolayers of the shorter homologues turned out to be homogeneous until their collapse, whereas for longer homologues, the formation of multilayer aggregates was observed. The methods of grazing incidence X-ray diffraction (GIXD) and X-ray reflectivity (XR) have also been applied for the characterization of the organization of thioether molecules in their monolayers. The GIXD experiments proved that the films of the studied thioethers possess a periodical in-plane structure. They are collectively tilted toward the next neighbor (NN tilt), and their packing within the monolayer (*xy*) plane can be described by the 2-dimentional rectangular centered lattice. Interpretation of the XR results indicate that only the partially fluorinated chain of the thioether molecule is periodically organized at the water/air interface, whereas the hydrocarbon chain is disordered and has a liquid character.

Introduction

Semifluorinated alkanes (SFAs) are diblock molecules of the general formula $C_mF_{2m+1}-C_nH_{2n+1}$ (often abbreviated as FmHn). Despite their structural simplicity, this class of chemicals has attracted considerable scientific interest, resulting in a plethora of scientific publications.[1,2] The scientific attractiveness of SFAs originates from their surface activity and ability to self-organize in different media, originating from the fact that two mutually phobic moieties (one hydrogenated and one perfluorinated) are covalently bound together.[3] SFAs do not have the structure of a typical surfactant molecule, containing usually a hydrophilic headgroup and a hydrophobic tail. In contrast, the entire SFA molecule is hydrophobic and devoid of any fragment that could serve as a headgroup, but both the mutual phobicity of both building blocks and considerable dipole moment originating from the $-CF_2-CH_2-$ junction can be considered as factors responsible for the above-mentioned surface activity.[4] SFAs self-organize in organic and fluorous media, forming different aggregates as micelles, reversed micelles, and vesicles.[5,6] Different representatives of SFAs have been reported as being capable of Langmuir monolayer formation. This has been widely studied since the early papers by Gaines, published in 1991.[7−10]

So far, the majority of studies have been done on SFA molecules without any structural modifications. There are some papers regarding SFAs containing halogen atoms, such as Br and I, introduced in the terminal position of the H-chain,[11] or discussing the influence of the iso branching of the F-chain on the physical properties of these molecules;[12] however, such reports are not numerous. On the other hand, semifluorinated chains are often applied as components of classical surfactants terminated with the −OH, −COOH or other polar headgroups. Such molecules have been frequently studied since the early investigations of Shafrin and Zisman[13−15] due to their more favorable properties as compared with hydrogenated surfactants.

Since the presence of the fluorinated chain in addition to the hydrogenated one in the molecule has been proved to lead to a plethora of interesting and beneficial properties, we have decided to proceed further and modify the structure of SFA molecule, maintaining its hydrophobic character. Our idea was to introduce a heteroatom into the SFA molecule to replace one $-CH_2-$ group in the H-chain. We decided to introduce sulfur and, thus, synthesize a homologous series of semifluorinated thioethers. Although there are some reports in the scientific literature regarding the synthesis of such compounds,[16−18] their physicochemical characterization has not been performed. Hydrogenated surfactants possessing thioether sulfur in the hydrophobic chain have also been studied.[19,20] It has been shown that the inclusion of one or two thioether groups along the hydrophobic tail retains the typical surfactant behavior; however, it has to be kept in mind that methylene and thioether groups are not directly interchangeable.[20]

The main objective of our studies was the investigation of the effects of the inclusion of one thioether sulfur atom into the semifluorinated alkane molecule on the physical properties of Langmuir monolayers formed by such chemicals. For this purpose, we have synthesized six homologous partially fluori-

* Corresponding author. Phone: +48126632082. Fax: +48126340515. E-mail: broniato@chemia.uj.edu.pl.
† Jagiellonian University.
‡ Los Alamos National Laboratory.

10.1021/jp105114d
Published on Web 09/14/2010

nated thioethers of the general formula $CF_3-(CF_2)_7-(CH_2)_{10}-S-C_nH_{2n+1}$, where $n = 1, 2, 4, 8, 12$, and 18. All these molecules have the same partially fluorinated chain consisting of 18 carbon atoms and differ in the length of the second hydrogenated chain. Although all the studied compounds are hydrophobic in nature, they differ in the location of the sulfur atom, which shifts from the terminal position (for $n = 1$) to the middle of the molecule (for $n = 18$).

It has already been proved that semifluorinated alkanes are oriented in Langmuir monolayers with the perfluorinated moiety toward the air,[7,8,10] and consequently, the same orientation can be assumed for the partially fluorinated thioethers. Therefore, for molecules with $n = 1$ and 2, the sulfur atom of the groups $-S-CH_3$ and $-S-C_2H_5$ remains close to the water/air boundary, whereas for longer analogues, it is located some distance away. The presence of thioether sulfur close to the water/air interface can have a profound effect on the properties of Langmuir monolayers formed by the investigated compounds because the groups $-S-CH_3$ and $-S-C_2H_5$ can be treated as a kind of a pseudoheadgroups in such molecules. On the other hand, the presence of the sulfur atom closer to the middle of the molecule may break the all-trans conformation of the hydrocarbon chain and introduce disorder in packing of the investigated molecules in Langmuir monolayers.

In our research, we have applied the classical Langmuir technique, in which the surface pressure (π)−mean molecular area (A) isotherms are registered. This technique provides the information about the ability of the investigated molecules to form Langmuir monolayers and, if so, about the stability of such films. To have an insight into electrical properties of the monolayers, the change of surface potential was monitored upon film compression (registration of $\Delta V-A$ isotherms). All the investigated monolayers have also been visualized with Brewster angle microscopy (BAM). To understand the organization of the thioether molecules within their monolayers, we applied the methods of X-ray scattering from such films. We have applied grazing incidence X-ray diffraction (GIXD) to obtain information about the lateral organization of the investigated monolayers and X-ray reflectivity (XR) measurements, which have provided information about the electron density distribution in the direction perpendicular to the air−water interface. GIXD and XR experiments turned out to be very effective tools in the discussion of the structure of the monolayers formed by semifluorinated alkanes and related molecules,[8,21,22] and we think that their application in our research of the films formed by partially fluorinated thioethers will shed new light on the organization of fluorinated molecules at interfaces.

Experimental Section

Materials. The investigated fluorinated thioethers are not commercially available and have been synthesized in our laboratory by one of us (M.B.). Perfluorooctyl iodide was purchased from Fluorochem. All other necessary chemicals for thioether synthesis and all solvents were supplied by Aldrich. Chloroform applied for the preparation of the spreading solutions was of spectroscopic purity (99.9%, stabilized by ethanol). Milli-Q ultrapure water (resistivity of 18.2 MΩ·cm) was applied in all Langmuir experiments.

Synthesis of Fluorinated Thioethers. All the investigated compounds have the following structure: $CF_3-(CF_2)_7-(CH_2)_{10}-S-C_nH_{2n+1}$, where $n = 1, 2, 4, 8, 12, 18$. Thus, all of them have the fluorinated chain identical and differ in the length of the second (hydrogenated) fragment. The systematic names of the investigated thioethers are complicated; therefore, depending on the length of the hydrogenated chain (n value), the following abbreviations have been acquired: FC1; FC2; FC4; FC8; FC12, and FC18 for $n = 1-18$, respectively. They were synthesized following the method described in the literature[23] in a reaction of an alkyl iodide with an alkyl thiol in the presence of cesium carbonate and tetrabutylammonium iodide as a catalyst:

$$RI + R'SH \xrightarrow[TBAI,DMF]{Cs_2CO_3} R-S-R'$$

Typically the iodide was $CF_3-(CF_2)_7-(CH_2)_{10}I$; only in the synthesis of the thioether FC1 were methyl iodide and $CF_3-(CF_2)_7-(CH_2)_{10}-SH$ applied.

The synthesis of the semifluorinated alcohol $CF_3-(CF_2)_7-(CH_2)_{10}-OH$ has been described in the scientific literature,[14] whereas the semifluorinated iodide was obtained from this molecule in the reaction with triphenylphosphine/iodine complex:[11]

$$CF_3-(CF_2)_7-(CH_2)_{10}-OH \xrightarrow[THF,\ CH_2CI_2]{P(Ph)_3,I_2} CF_3-(CF_2)_7-(CH_2)_{10}-I$$

The structure and purity of the synthesized thioethers was proved by ^1H, ^{13}C NMR, elemental analysis, mass spectroscopy and IR spectra. The purity of the synthesized chemicals was estimated to be higher than 99%.

Methods

Surface Pressure Isotherms Registration. The $\pi-A$ isotherms of the investigated compounds have been registered on the NIMA 611 double barrier trough or on the NIMA 601 double barrier trough (BAM experiments) (NIMA, Coventry, UK). The surface pressure was monitored continuously by Wilhelmy electronic microbalance with an accuracy of 0.1 mN/m, using filter paper made of Whatman ashless chromatographic paper as the pressure sensor. Samples of the investigated fluorinated thioethers were dissolved in chloroform (Aldrich, spectroscopic purity). In every experiment, $\sim 5 \times 10^{16}$ molecules were spread from the chloroform solution by a Hamilton microsyringe onto the surface of ultrapure water. At least 10 min was allowed for solvent evaporation, and then the compression was started at a compression rate of 20 cm^2/min (~ 2 $Å^2$/molecule·min^{-1}) because it turned out that a compression rate up to 50 cm^2/min does not exert adverse effects on the isotherm characteristics. The subphase temperature was controlled with the Julabo water circulating bath with accuracy of 0.1 °C. All the experiments were carried out at room temperature. All the $\pi-A$ isotherms presented herein are averages of at least three measurements.

Surface Potential Measurements. Surface potential measurements were performed with the vibrating capacitor method (Kelvin probe). The instrument was produced by KSV (KSV-Spot, KSV, Helsinki, Finland) and mounted on a NIMA 611 trough. The vibrating plate was located ~ 2 mm above the water subphase. The instrument has an accuracy of ± 5 mV. The $\Delta V-A$ curves for a particular thioether were repeated at least three times, and the resultant curves presented in the results are averages of the measurements.

Brewster Angle Microscopy Observations. A Brewster angle microscope, BAM 2 plus (NFT, Germany), was used for microscopic visualization of the monolayer structure. It is equipped with a 50 mW laser, emitting p-polarized light of 532 nm wavelength, which is reflected off the air−water interface

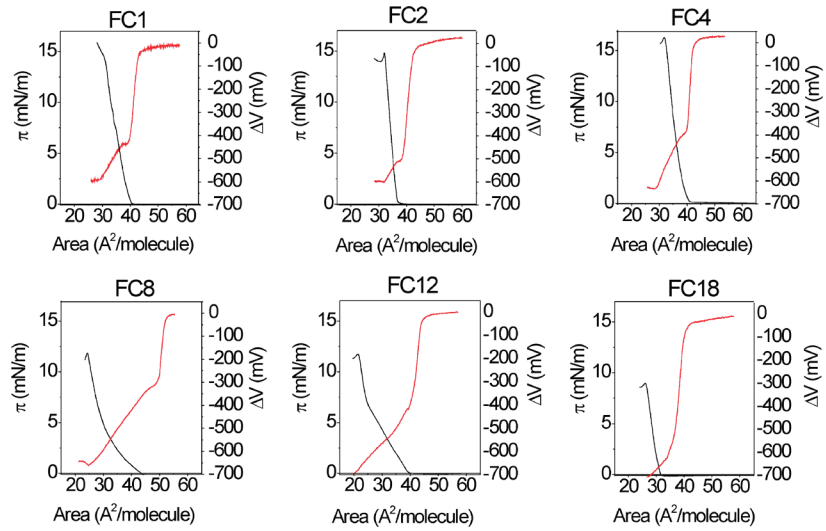

Figure 1. Surface pressure−mean molecular area (π−A) (black curves) and surface potential−mean molecular area (ΔV−A) (red curves) isotherms of the investigated partially fluorinated thioethers.

at ~53.15° (Brewster angle). All the applied equipment was placed on an antivibration table. The lateral resolution of the microscope was 2 μm. The images were digitized and processed to obtain the best quality BAM pictures. Each image corresponds to a 770 μm × 570 μm monolayer fragment.

X-ray Scattering Methods.

GIXD Experiments. All the X-ray scattering experiments were performed in DESY, Hasylab, Hamburg, Germany. The theoretical foundations of grazing incidence X-ray diffraction and the liquid diffractometer applied here have been described previously.[24−26] GIXD experiments were carried out to obtain the information about the lateral ordering in the monolayers formed by the investigated molecules. The scattered intensity is measured by scanning over a range of horizontal scattering vectors, Q_{xy}:

$$Q_{xy} \approx \frac{4\pi}{\lambda} \sin(2\theta_{xy}/2)$$

where $2\theta_{xy}$ is the angle between the incident and diffracted beam projected on the liquid surface. The GIXD intensity resulting from a powder of 2D crystallites can be represented as Bragg peaks, resolved in the Q_{xy} direction, by integrating the scattered intensity over all the channels of the position-sensitive detector, perpendicular to the interface defined as the Q_z direction. Conversely, the Bragg rod profiles were resolved in the Q_z direction and obtained by integrating the scattered intensity over Q_{xy} corresponding to the Bragg peak. The angular positions of the Bragg peaks determine the d spacing, $d = 2\pi/Q_{xy}^{max}$ (where Q_{xy}^{max} is the position of the maximum of Bragg peak along the Q_{xy}) for the 2D lattice. From the line width of the Bragg peak, it is possible to determine the 2D crystalline coherence length, L_{xy}, the average distance in the direction of the reciprocal lattice vector, Q_{xy}, over which the ordering extends. The intensity distribution along the Bragg rod can be analyzed to determine the magnitude and direction of the molecular tilt and the coherently scattering length (L_z) of the molecule measured along its backbone.

X-ray Reflectivity Experiments. To minimize the beam damage during X-ray reflectivity measurements, the monolayer sample was occasionally translated in the horizontal plane, perpendicular to the beam. This was achieved by moving the trough by 2 mm, which corresponded to a full width of the beam in the horizontal plane. Rerecording of the reflectivity curve before and after such translation afforded a check of the reproducibility.

In X-ray reflectivity, detailed information about the laterally averaged, out-of-plane, electron density distribution in a film can be obtained by modeling the deviation of the measured specular X-ray reflectivity from the Fresnel's curve (R_F) obtained for an ideally sharp interface.[27,28] With identical incident (α_i) and reflected (α_f) angles, $\alpha_i = \alpha_f = \alpha$, the X-ray reflectivity curve $R(Q_z)$ can be measured by a NaI scintillation detector moving on the α_f arc. The variable Q_z is the momentum transfer defined as

$$Q_z \approx \frac{2\pi \sin(\alpha)}{\lambda}$$

where λ is the wavelength of the X-ray beam. The absolute reflectivity data were obtained by subtracting the measured background and normalizing the measured reflectivity $R(Q_z)$ with respect to the incident flux.

By assuming that a homogeneous electron density, $\rho(z)$, is laterally averaged over the footprint of the beam, an electron density model can be built with a stack of homogeneous slabs ("boxes"). Each box is assumed to have a constant electron density and thickness. The interfaces between the boxes are smeared out using a Gaussian function with a standard deviation, σ, to account for the roughness at the boundaries due to the thermally excited capillary waves and atomic roughness of the interface[29,30]

Simulations of the reflectivity profiles were performed with the Parratt32 software package (Hahn−Meitner Institute, Berlin). In this package, the calculation of reflectivity of X-rays was based on Parratt's recursive algorithm for stratified media using independent layers.[31] Parameters in the least-squares fitting procedure of the experimental data were the electron density and thickness of each box as well as the roughness parameters between adjacent boxes.

Results and Discussion

Figure 1 presents the surface pressure−mean molecular area (π−A) and surface potential−mean molecular area (ΔV−A)

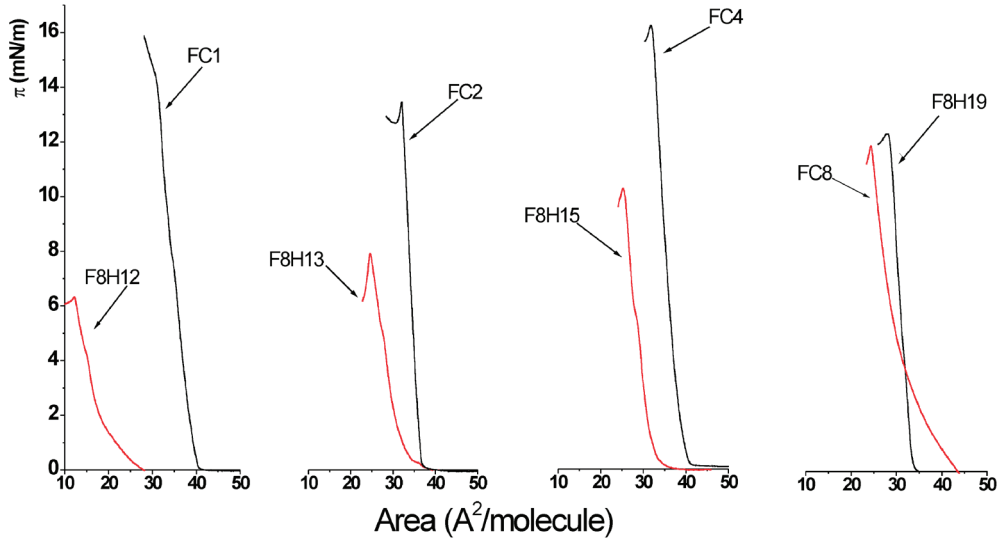

Figure 2. Surface pressure−mean molecular area ($\pi-A$) isotherms of the selected partially fluorinated thioethers (black curves) compared with the $\pi-A$ isotherms of semifluorinated alkanes of the F8 series (red curves).

isotherms for the investigated six thioethers. It turns out that all the investigated compounds are capable of Langmuir monolayer formation when spread from chloroform solution at the air/water interface. The liftoff area of the isotherms is ∼40 Å^2/molecule, except for FC18, for which the surface pressure rise begins at a lower value. The isotherms of FC1, FC2, and FC4, the compounds with short second hydrocarbon chain, are steep and collapse (π_C) at ∼15 mN/m and at the molecular area of ∼32 Å^2/molecule. The $\pi-A$ isotherms of FC8 and FC12 are less steep, and the films collapse at ∼12 mN/m, which is a slightly lower value than observed for the thioethers with shorter hydrocarbon chain.

Moreover, in the course of the $\pi-A$ isotherm of FC12, a phase transition is manifested as the change in the isotherm inclination angle observed at ∼7 mN/m. The $\pi-A$ isotherm of FC18 is visibly shifted to lower molecular areas as it lifts off at ∼32 Å^2/molecule and collapses at ∼27 Å^2/molecule, and the collapse pressure is only 9 mN/m. As stated in the Introduction, partially fluorinated thioethers can be treated as modified semifluorinated alkanes, in which one $-CH_2-$ group was exchanged by the sulfur atom. Therefore, it is of interest to compare the isotherms of partially fluorinated thioethers and SFAs of the same length and the same degree of the hydrocarbon chain fluorination (the F8 series). In such an attempt, FC1 corresponds to F8H12, FC2 to F8H13, FC4 to F8H15, and FC8 to F8H19. We are unable to compare FC12 and FC18 with the corresponding SFAs because the data in literature is accessible only for SFAs from the F8 series with no more than 20 carbon atoms in the hydrocarbon moiety.[32] The compared isotherms are shown in Figure 2.

It can be observed that the $\pi-A$ monolayer of F8H12 collapses at 6 mN/m and the lift-off area of the isotherm is ∼30 Å^2, which distinguishes profoundly this compound from FC1 monolayers. Moreover, F8H12 is known to form very unstable monolayers,[32] in contrast to FC1, which forms stable films at the air/water interface. Thus, in this case, the presence of the sulfur atom is clearly manifested in the surface properties of similar substances. FC1 is terminated with the $S-CH_3$ group, meaning that the sulfur atom remains in the interfacial region, in contact with water molecules. The electronegativity of sulfur is comparable with carbon; however, the difference is in the electron density distribution. Sulfur possesses two free electron pairs that are not present on the carbon in the $-CH_2-$ group.

The interactions of the free electron pairs with water molecules can be the key factor responsible for the stability of the monomolecular films formed by FC1 at the air/water interface. Moreover, it was proved that thioether sulfur can form hydrogen bonds.[33−35] They are rather weak, but their formation can elucidate the observed stabilizing effect of the presence of the $-S-CH_3$ or $-S-C_2H_5$ groups in the investigated thioethers. The same arguments can be applied when comparing the isotherms of FC2 and F8H13. However, the trend is different for longer thioethers. FC4 has a higher collapse pressure than F8H15; however, the isotherms have very similar inclination and a comparable course. As far as the isotherms of FC8 and F8H19 are concerned, they have similar collapse pressures, but the isotherm of FC8 is visibly more expanded.

A general conclusion can be drawn from the discussed comparison that the surface properties of fluorinated thioethers depend considerably on the location of the sulfur atom within the molecule. If sulfur is close to the terminus of the molecule, as in the groups $-S-CH_3$ and $-S-CH_2-CH_3$, it can have a direct contact with water molecules. The interactions are attractive because the location of two free electron pairs on the sulfur atom, which, in consequence, leads to the increase in surface activity of the chemicals and to the higher stability of Langmuir monolayers at the air/water interface. In FC4, the sulfur atom is not in the terminal position preceeded by the butyl group but still, because of the roughness of the interface, can have some contact with water molecules that may improve the properties of Langmuir monolayers as compared with the SFAs of the same length. However, for longer thioethers investigated here, the sulfur atom is shifted toward the middle part of the molecule, and its possible interaction with water molecules ceases to be important.

The surface potential−mean molecular area ($\Delta V-A$) isotherms are included in Figure 1. Similarly, to other fluorinated surfactants,[36,37] the sign of the surface potential is negative. The surfaces potential starts to change (decrease) at higher mean molecular areas than the lift-off of the respective $\pi-A$ isotherms. Such a trend is commonly observed for different surfactant classes because the organizing effect of the film compression is earlier observable in electrical than mechanical properties due to the fact that surface potential is very sensitive to any change in the organization of the dipole moments. For all the studied molecules, the course of the surface potential curve is very

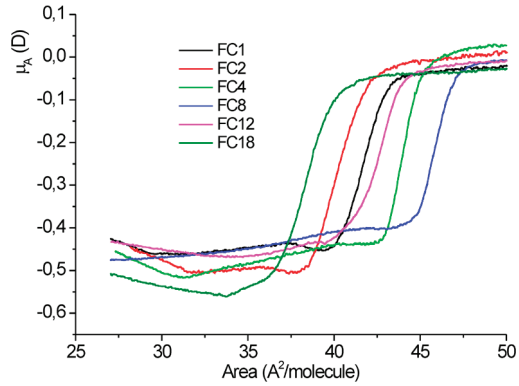

Figure 3. Apparent dipole moment−mean molecular area (μ_A−A) isotherms for the investigated partially fluorinated thioethers.

similar. It starts to decrease at ∼50−45 Å^2/molecule, falling rapidly to a value of ∼ −500 mV where it achieves a kind of a shallow plateau. This plateau corresponds to the beginning of the surface pressure rise. The compression of the monolayers leads to a further decrease in the surface potential value. The above-mentioned plateau is only weakly marked in the ΔV−A isotherm of FC12 and practically not present for FC18.

To have a deeper insight into the electrical properties of the investigated monolayers, the apparent dipole moment (μ_A)−mean molecular area (A) isotherms have been calculated. Partially fluorinated thioethers are molecules devoid of any ionizable group, which cannot acquire an electrical charge on them at any pH value. Especially at ∼5.5 (the pH of Milli-Q water), the investigated molecules are not ionized. Therefore, the surface potential can be modeled applying the so-called Helmholtz approach, proposed originally by Davies and Rideal.[38,39] In this model, the surface potential change (ΔV) is related to the vertical component of the dipole moment of the film forming molecules ($\mu_\perp$) with the following formula:

$$\Delta V = \frac{\mu_\perp}{A\varepsilon\varepsilon_0}$$

where A is the mean molecular area, ε_0 is the vacuum permittivity, and ε is the permittivity of the monolayer. Because the monolayer permittivity (ε) is not known, the quotient $\mu_\perp/\varepsilon$ is often substituted by the symbol μ_A, called apparent dipole moment. The μ_A−A isotherms are presented in Figure 3.

As can be seen, the μ_A−A isotherms have virtually the same characteristic for all the investigated molecules. After a rapid fall, the μ_A value stabilizes at ∼ −0.5 D at a mean molecular area corresponding to the initial region of the π−A isotherm. It means that the collective orientation of molecules is established at low surface pressures (the collective tilt), and their orientation remains unchanged upon further compression. Such an interpretation can be accepted taking into consideration the range of relatively low surface pressures, where the monomolecular layer exists.

The dipole moments have been calculated for the investigated molecules using the Hyperchem Package.[40] It turns out that the dipole moments calculated in vacuum are nearly identical for all the investigated thioethers, ranging from 2.8 to 2.9 D. This is understandable because the main contribution to the dipole moment in this case originates from the $-CF_2-CH_2-$ connection, some additional contributions are carried by the terminal $-CF_3$ and $-CH_3$ groups,[41] and probably some small contribution may come from the −S− linkage, especially because of the asymmetry of the whole molecule. All the above-mentioned elements are present in the investigated molecules, so it is not surprising that the calculated dipole moments are the same within the range of error.

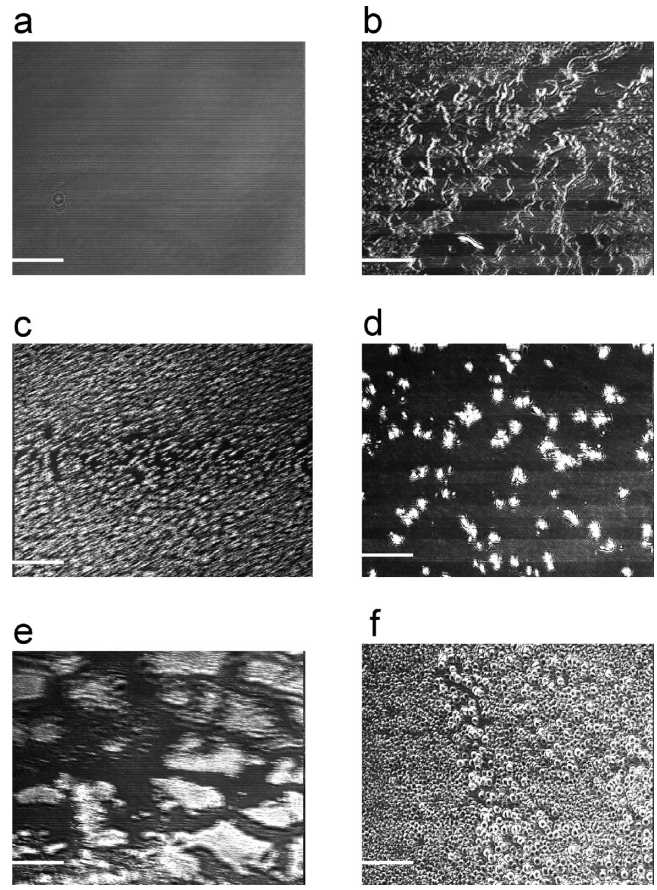

Figure 4. Representative BAM images for the investigated monolayers. (a, b) FC2: a, π = 10 mN/m; b, π = 14 mN/m. (c, d) FC12: c, π = 4 mN/m; d, π = 9 mN/m. (e, f) FC18: e, π = 4 mN/m; f, π = 9 mN/m. White bars in the photos corresponds to 100 μm.

The value of 2.8 D is typical for different semifluorinated alkanes,[10,32] and the fact that it is also observed for the partially fluorinated thioethers means that the contribution from the −S− linkage is negligible and that the molecule is probably not bent at the −S− linkage. It was also revealed by the Hyperchem simulations that the dipole moment vector is not parallel to the molecular backbone. A similar situation was observed for semifluorinated alkanes,[42] in which the angle between the molecular backbone and the dipole moment was estimated to be 35°. As was stated above, the contribution of the thioether sulfur into the dipole moment in the investigated thioethers is negligible, so it can be assumed that here, the angle between the backbone and the dipole moment is the same. Therefore, the maximum value of μ_A can be achieved when the thioether molecules remain collectively tilted from the normal of the monolayer and when the tilt angle is 35°. The value of the tilt angle can be verified by GIXD and will be discussed later.

All the investigated monolayers have been visualized upon their compression with Brewster angle microscopy, and the representative BAM images are presented in Figure 4.

Figure 4a and b illustrates the BAM images upon compression of FC2. The behavior of FC1, FC4, and FC8 films was identical, as far as the visualization of their films is concerned. At the beginning of compression at mean molecular areas much larger than the lift-off of the π−A isotherm, the films are completely

homogeneous. At the lift-off area and upon following compression, no changes have been observed (Figure 4a). The monolayers remained homogeneous until the collapse pressure. At collapse, white spots and longer stripes appeared rapidly in BAM images (Figure 4b), proving the formation of multilayer structures within the films.

The monolayers formed by FC12 behave differently. At surface pressures corresponding to the lift-off of the $\pi-A$ isotherm, a large number of small gray domains can be observed at the water/air interface. They can be interpreted as domains of a liquid phase in equilibrium with the less organized gaseous phase of the visualized monolayer. At ~6 mN/m at the surface pressure corresponding to the change of inclination of the FC12 $\pi-A$ isotherm, numerous white spots appear. Such bright spots can be interpreted as the manifestation of the 3D phase formation, meaning that the collapse of FC12 films begins at surface pressures lower than 12 mN/m (collapse pressure of FC12 monolayers). Therefore, it can be noticed that the elongation of the hydrocarbon chain in a partially fluorinated thioether increases the propensity of the investigated molecules to aggregation and limits their film-forming properties. Long chain alkanes were also reported to form organized films at the air/water interface;[43] however, for such chemicals, aggregation is always a phenomenon that competes with the spreading at the water/air interface.

Finally, the monolayers of FC18 have been observed by the BAM microscope. The films behave differently from that of the shorter homologues. At low surface pressures corresponding to the lift-off of the $\pi-A$ isotherms, large islet-like domains of a condensed phase can be observed (Figure 4e) Upon film compression, they come in closer contact, and at a π_C of ~9 mN/m, a great number of small 3D nuclei can be seen in the BAM photos (Figure 4f). The lift-off area of the $\pi-A$ isotherms of FC18 is noticeably lower than for the other investigated thioethers, which together with the appearance of the condensed domains in the BAM images means that the large length of FC18, which is an analogue of a 37-carbon-atom alkane heptatriacontane, has an organizing effect on the investigated film. The driving force for the formation of Langmuir monolayers of such nontypical compounds as long chain alkanes is the van der Waals forces.[44] However, the same forces are responsible for the aggregation of such compounds. This competition is reflected in the relatively low collapse pressure of the FC18 monolayer and the formation of 3D nuclei visualized in Figure 4f.

To have insight into the organization of the investigated molecules within their monolayers, we have applied the methods of the synchrotron X-ray scattering; namely, GIXD and XR measurements. For these studies, we have selected two of the investigated thioethers: FC2 as a representative of the compounds with a shorter hydrogenated chain and FC18 as the longest of the investigated molecules and also a compound that forms large, condensed domains in monolayers as visualized with BAM. We would like to start from the presentation and discussion of the GIXD data. The monolayer of CF2 was compressed to 10 mN/m, whereas the film of FC18 was compressed to 7.5 mN/m. The compression was stopped, and the surface pressure was held constant during the GIXD experiment. The GIXD data are presented in Figure 5 as Bragg peaks (intensity versus Q_{xy}) and Bragg rods (intensity versus Q_z).

As can be seen in Figure 5, it was possible to register Bragg peaks for both monolayers, which corroborates the periodicity of the lateral ordering of the molecules. The Bragg peaks

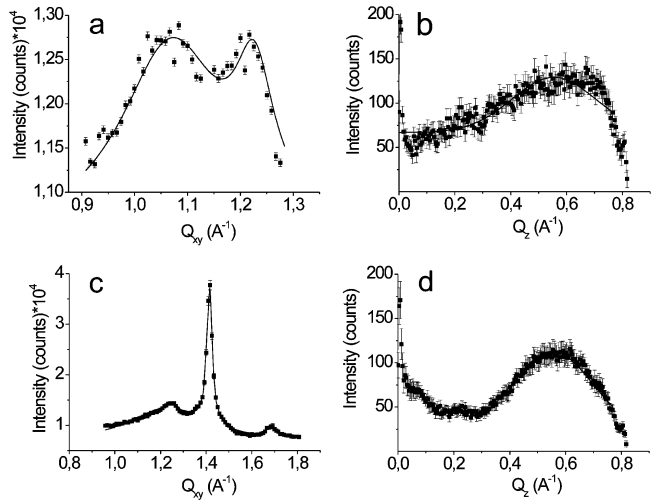

Figure 5. GIXD data for the selected partially fluorinated thioethers: (a) Bragg peak for FC2, (b) Bragg rod for FC2, (c) Bragg peak for FC18, (d) Bragg rod for FC18. The solid lines were fitted to Bragg peaks using Voigt functions.[25]

observed for FC2 and FC18 differ in intensity but have similar characteristics. In both cases, two distinct maxima can be observed. The presence of two maxima in the $I(Q_{xy})$ plot results from the deformation of the hexagonal unit cell caused by the collective tilt of the film, forming molecules from the monolayer normal. The lattice can be represented as rectangular-centered. The calculated d spacings in the (11) and (02) directions and the lattice parameters are gathered in Table 1. An additional low-intensity maximum at ~1.7 Å^{-1} can be noticed in the Bragg peak for FC18 (Figure 5c). It can originate from the presence of some 3D crystallites of the substance present in the monolayer since, as was discussed before for the case of long-chain, nontypical surfactants aggregation competes with spreading.

In both cases, the Bragg rods (Figure 5b and d) have two maxima: one at 0 Å^{-1} and the second at ~0.55 Å^{-1}. Such a situation is typical for a monolayer formed by tilted molecules[45] in a rectangular centered lattice. The width of the peak centered at 0.55 Å^{-1} measured at half-maximum enables one to estimate the coherence length of the scattering molecule, L_z. It is 18.8 ± 1.5 Å for FC2 and 19.4 ± 1 Å for FC18, meaning that L_z for both compounds is identical within the limit of error. It is very important information: both compounds differ profoundly in their structure because FC18 has the hydrogenated chain 16 carbon atoms longer than FC2. L_z is not a measure of the monolayer thickness or the length of the entire molecule; it is the length of this part of the molecule measured along the molecular backbone, which scatters coherently. Both molecules have the same partially fluorinated chain: $CF_3-(CF_2)_7-(CH_2)_{10}-$. The length of the chain can be calculated to be 24 Å.[46] It can be inferred from the GIXD data that the molecules are tilted toward the next neighbor (NN), and from the exact location of the second maximum of the Bragg rods, it can be calculated that the tilt of FC2 molecules is $\tau \approx 30°$; for FC18, $\tau \approx 26°$.

The value of the tilt angle agrees well with the value estimated from the discussion of the dipole moments, which was estimated to be ~35°.

The observed L_z values are shorter than 24 Å, which can originate from the disordering of the $-CH_2-$ groups bound to the sulfur atom or from the thermal movement of the terminal $-CF_3$ group. The most important conclusion from this part of our experiments is that the hydrogenated chains of the inves-

TABLE 1: Structural Parameters Obtained from the GIXD Data

name	d spacing (Å) ± 0.005	lattice parameters	L_z (Å)	L_{xy} (Å)	A (Å^2/molecule)
FC2	$d_{11} = 5.88$ $d_{02} = 5.12$	$a = 7.18$ Å; $b = 10.24$ Å $\gamma = 109.9°$ tilt, $\tau = 28.9°$	18.8 ±1.5	$L_{11} = 24 \pm 3.5$ $L_{02} = 71 \pm 9$	36.76
FC18	$d_{11} = 5.12$ $d_{02} = 4.44$	$a = 6.21$ Å; $b = 8.88$ Å $\gamma = 110.0°$ tilt, $\tau = 25.5°$	19.4 ±1	$L_{11} = 14 \pm 0.8$ $L_{02} = 200 \pm 5$	27.57

tigated thioethers are not periodically ordered. In the case of FC2, the fragment $-S-C_2H_5$ can be treated as a kind of a headgroup, and it is known from previous studies that headgroups are usually not periodically ordered in Langmuir monoalyers.[45] However, as discussed above, FC18 resembles the 37-carbon-atom alkane heptatriacontane because it is impossible to distinguish any headgroup in its structure. Therefore, the GIXD data prove that a part of this monolayer-forming molecule, namely, the partially fluorinated chain, is periodically ordered, and the rest of the molecule, the hydrogenated chain, is disorganized, probably forming a liquid structure.

The normalized reflectivity curves (multiplied by Q_z^4) are presented in Figure 6.

To find the best fit of the experimental reflectivity data, the reflectivity was modeled applying the Parratt algorithm.[31] It is logical to divide the partially fluorinated thioether molecule into three boxes of constant electron density: one box of high electron density containing the perfluorinated fragment of the molecule, a second box of low electron density containing the hydrogenated fragment of the partially fluorinated chain, and a third box of moderate electron density (as compared with bulk water) containing the disordered hydrogenated chain. Surprisingly, such an approach did not lead us to any reasonable models, because the values of χ^2 of such models were unacceptably high. Therefore, we tried to model the reflectivity with a double-box model. In this approach, the $CF_3-(CF_2)_7-$ moiety is described by the first box of high electron density, and the $-(CH_2)_9-$ fragment is in a second box of low electron density. In such an approach, the whole fragment, $-CH_2-S-C_2H_5$ for CF2 and $-CH_2-S-C_{18}H_{37}$, is disregarded. We omit these fragments in our consideration, assuming that they have electron density similar to bulk water. Such an approach led us to reasonable fits of the experimental reflectivity data and low χ^2 values. The lengths of the boxes, electron densities, numbers of electrons in a box, and the roughness at the box boundary are shown in Table 2. The resultant electron density profiles are shown for FC2 in Figure 7 and for FC18 in Figure 8.

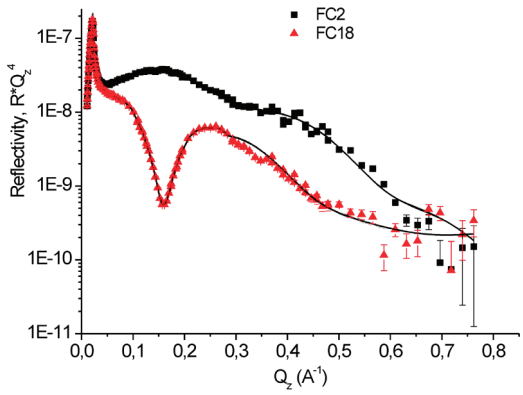

Figure 6. Normalized X-ray reflectivity curves measured for the monolayers of FC2 (solid squares) and FC18 (solid triangles). The solid lines are the fits using the models shown in Table 2.

On the basis of the reflectivity modeling and the above discussion of the GIXD data, the models of the organization of the FC2 and FC18 molecules within their monolayers have been proposed and are presented in Figures 7 and 8, respectively. The molecules of FC2 are collectively tilted in their monolayers 30° from the monolayer normal. The fragment $CF_3-(CF_2)_7-(CH_2)_9-$ is periodically in-plane-ordered, forming a rectangular-centered 2D lattice. The statistical surface domain contains ~120 molecules (estimated from the L_{xy} value in the (02) direction; see Table 1). The fragment $S-C_2H_5$ can be treated as a kind of

TABLE 2: The Results of the XR Analysis[a]

	box 1 (tail)					box 2 (head)				
name	length (Å)	SLD, ρ (Å^{-2}) × 10^{-6}	σ (Å)	e$^-$ in box	e$^-$ calcd	length (Å)	SLD, ρ (Å^{-2}) × 10^{-6}	σ (Å)	e$^-$ in box	e$^-$ calcd
FC2	9.28	16.40	3.2	201	199	9.24	5.64	2.9	72	69
FC18	10.0	19.30	3.1	201	198	10.2	6.68	3.4	72	70

[a] Box models of the electron density distribution along the z axis for the investigated monolayers are shown.

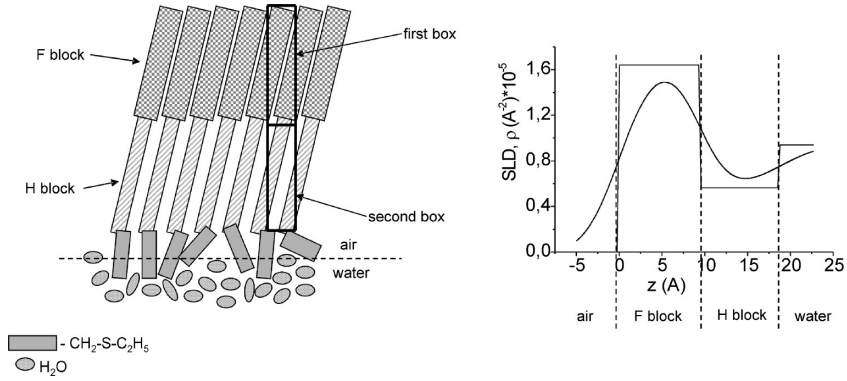

Figure 7. Electron density profile and the schematic representation of the organization of the FC2 molecules at the water/air interface.

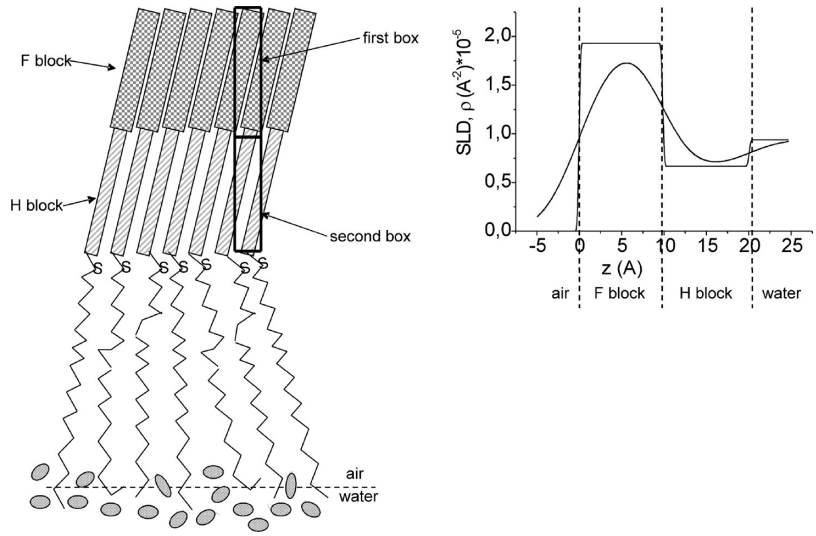

Figure 8. Electron density profile and the schematic representation of the organization of the FC18 molecules at the water/air interface.

a headgroup in contact with water molecules. This fragment is disordered and has a different orientation at the air/water interface, indicating that the torsion angle in the fragment C−S−C−C is not fixed. The electron density in the headgroup sublayer is similar to the electron density of the bulk water subphase, which is also caused by the penetration of water molecules into the headgroup sublayer.

Similar considerations have been undertaken for FC18. The resultant scheme of the molecular organization within the Langmuir monolayer is drawn in Figure 8. Similar to FC2, in the monolayer of FC18, the partially fluorinated chain is laterally periodically ordered. The statistical surface domain contains ∼1100 molecules (estimated from the L_{xy} value in the 02 direction; see Table 1). It means that a statistical surface domain of FC18 contains ∼10 times more molecules than in the case of FC2. This can find its manifestation in the large condensed domains visible in BAM images and also in the relatively high intensity of the scattered X-ray radiation. The fragment $-S-C_{18}-H_{37}$ is regarded as in the liquid state. It is underlined at the scheme by the different orientation of this moiety and by the presence of multiple gauche defects schematically pointed out in Figure 8. The important observation here is the fact that although the long $-S-C_{18}H_{37}$ fragment is disordered, the mutual van der Waals interactions between the chain cause stronger intermolecular interactions, which is reflected in the larger size of the surface domains.

Conclusions

All the investigated partially fluorinated thioethers are capable of the Langmuir monolayer formation. For the homologues with a short second hydrocarbon chain (as $-S-CH_3$ and $-S-C_2H_5$), the terminal fragment can be regarded as a kind of headgroup anchoring the molecule at the water/air interface. This is proved by the fact that Langmuir monolayers of such thioethers exhibit considerably higher stability than the films formed by semifluorinated alkanes of identical length and degree of fluorination. For higher homologues, the thioether sulfur atom is shifted farther from the interface toward the air and has no contact with water molecules. In such molecules, the S atom replacing a $-CH_2-$ group does not stabilize the monolayers and is, rather, a source of additional disorder in the hydrophobic chain. Similar to other groups of fluorinated surfactants, partially fluorinated thioethers exhibit a negative change of surface potential upon compression. The virtually identical course of the apparent dipole moment (μ_A)−mean molecular area (A) curves observed for all the investigated compounds prove that their orientation at the water/air interface is very similar, regardless the length of the second (hydrogenated) chain. BAM microscopy observations proved that the monolayers of shorter homologues of the investigated series are homogeneous until the monolayer collapse, whereas the elongation of the second hydrocarbon chain and, consequently, the shift of the sulfur atom toward the middle of the molecule increases the propensity of the thioether molecule to aggregate and, as a result, decreases the stability of the Langmuir monolayer. The GIXD experiments performed on monolayers from two representatives of the investigated series corroborate the periodical arrangement of the molecules in the monolayer plane. The modeling of the out-of-plane orientation of the molecules (interpretation of the reflectivity curves) leads us to the conclusion that only the partially fluorinated chain of the thioethers is periodically ordered, whereas the second hydrogenated chain has a disordered character resembling melted long-chain hydrocarbons.

References and Notes

(1) Krafft, M. P.; Riess, J. G. *Chem. Rev.* **2009**, *109*, 1714–1792.
(2) Broniatowski, M.; Dynarowicz-Łatka, P. *Adv. Colloid Interface Sci.* **2008**, *138*, 63–83.
(3) Turberg, M. P.; Brady, J. E. *J. Am. Chem. Soc.* **1988**, *110*, 7797–7801.
(4) Kirsch, P. *Modern Fluoroorganic Chemistry*; Wiley-VCH: Weinheim, 2004.
(5) Lo Nostro, P. *Adv. Colloid Interface Sci.* **1995**, *56*, 245–287.
(6) Binks, B. P.; Fletcher, P. D. I.; Kotsev, S. N.; Thompson, R. L. *Langmuir* **1997**, *13*, 6669–6682.
(7) Gaines, G. L., Jr. *Langmuir* **1991**, *7*, 3054–3056.
(8) Huang, Z.; Acero, A. A.; Lei, N.; Rice, S. A.; Zhang, Z.; Schlossman, M. L. *J. Chem. Soc., Faraday Trans.* **1996**, *92*, 545–552.
(9) Broniatowski, M.; Dynarowicz-Ł£atka, P. *J. Fluorine Chem.* **2004**, *125*, 1501–1507.
(10) Broniatowski, M.; Sandez Macho, I.; Miñones, J., Jr.; Dynarowicz-Łatka, P. *Appl. Surf. Sci.* **2005**, *246*, 342–347.
(11) Wang, J.; Ober, C. K. *Liq. Cryst.* **1999**, *26*, 637–648.
(12) Broniatowski, M.; Dynarowicz-Łatka, P. *J. Colloid Interface Sci.* **2006**, *299*, 916–923.
(13) Shafrin, E. G.; Zisman, W. A. *J. Phys. Chem.* **1962**, *66*, 740–748.
(14) Broniatowski, M.; Dynarowicz-Łatka, P. *J. Colloid Interface Sci.* **2006**, *301*, 315–322.
(15) Kissa, E. *Fluorinated Surfactants and Repellents*; Marcel Dekker: New York, 2001.

(16) Huang, W.; Chunyang, J.; Derzon, D. K.; Huber, T.; Last, J. A.; Provencio, P. P.; Gopalan, A. S.; Dugger, M.; Sasaki, D. Y. *J. Colloid Interface Sci.* **2004**, *272*, 457–464.
(17) Crich, D.; Neelamkavil, S. *Org. Lett.* **2002**, *4*, 4175–4177.
(18) Szonyi, F.; Cambon, A. *J. Fluorine Chem.* **1989**, *42*, 59–68.
(19) Lundberg, D.; Shi, L.; Menger, F. M. *Langmuir* **2008**, *24*, 4530–4536.
(20) Menger, F. M.; Shei, L. *J. Am. Chem. Soc.* **2006**, *128*, 9338–9339.
(21) Krafft, M. P.; Giulieri, F.; Fontaine, P.; Goldmann, M. *Langmuir* **2001**, *17*, 6577–6584.
(22) Maaloum, M.; Muller, P.; Krafft, M. P. *Angew. Chem., Int. Ed.* **2002**, *41*, 4331–4334.
(23) Salvatore, R. N.; Smith, R. A.; Nischwitz, A. K.; Gavin, T. *Tetrahedron Lett.* **2005**, *46*, 8931–8935.
(24) Majewski, J.; Popovitz-Biro, R.; Bouwman, W. G.; Kjaer, K.; Als-Nielsen, J.; Lahav, M.; Leizerowitz, L. *Chem.—Eur. J.* **1995**, *1*, 304–311.
(25) Jensen, T. R.; Kjaer, K. Structural properties and interactions of thin films at the air−liquid interface explored by synchrotron X-ray scattering. *Novel Methods to Study Interfacial Monolayers*; Mobius D., Miller, R., Eds.; Elsevier: Amsterdam, 2001, Vol. 11; pp 205−254.
(26) Als-Nielsen, J.; Jacquemain, D.; Kjaer, K.; Leveiller, F.; Lahav, M.; Leiserowitz, L. *Phys. Rep.* **1994**, *246*, 251–313.
(27) Born, M.; Wolf, E. *Principles of Optics*; Pergamon Press: Oxford, 1984.
(28) Wu, D. G.; Malec, A. D.; Majewski, J.; Majda, M. *Electrochim. Acta* **2006**, *51*, 2237–2246.
(29) Braslau, A.; Deutsch, M.; Pershan, P. S.; Weiss, A. H.; Als-Nielsen, J.; Bohr, J. *Phys. Rev. Lett.* **1985**, *54*, 114–117.
(30) Pershan, P. S. *Faraday Discuss.* **1990**, *89*, 231–245.
(31) Parrat, L. G. *Phys. Rev.* **1954**, *95*, 359–369.
(32) Broniatowski, M.; Sandez-Macho, I.; Dynarowicz-Łatka, P. *Thin Solid Films* **2005**, *493*, 249–257.
(33) Spencer, J. N.; Harner, R. S.; Freed, L. I.; Penturelli, C. D. *J. Phys. Chem.* **1975**, *79*, 332–335.
(34) Doerksen, R. J.; Chen, B.; Liu, D.; Tew, G. N.; DeGrado, W. F.; Klein, M. L. *Chem.—Eur. J.* **2004**, *10*, 5008–5016.
(35) Jeffrey, G. A. *An Introduction to Hydrogen Bonding*; Oxford University Press: Oxford, 1997.
(36) Shibata, O.; Krafft, M. P. *Langmuir* **2000**, *16*, 10281–10286.
(37) Nakahara, H.; Nakamura, S.; Kawasaki, H.; Shibata, O. *Colloids Surf. B* **2005**, *41*, 67–80.
(38) Davies, J. T.; Rideal, E. K. *Interfacial Phenomena*, 2nd ed.; Academic Press: New York, 1963.
(39) Oliveira, O. N., Jr.; Bonardi, C. *Langmuir* **1997**, *13*, 5920–5924.
(40) *HyperChem Professional Release 5.1, A Molecular Visualization and Simulation Software Package*; Hypercube Inc.: Gainesville, FL, 1998.
(41) Araki, K.; Satoh, K.; Kondo, S. *Mol. Cryst. Liq. Cryst.* **1996**, *281*, 123–134.
(42) Broniatowski, M.; Sandez Macho, I.; Miñones, J., Jr.; Dynarowicz-Łatka, P. *J. Phys. Chem. B* **2004**, *108*, 13403–13411.
(43) Sirota, E. B. *Langmuir* **1997**, *13*, 3849–3859.
(44) Li, M.; Acero, A. A.; Huang, Z.; Rice, S. A. *Nature* **1994**, *367*, 151–153.
(45) Lang, P. Amphiphiles at Interfaces Studied by Surface-Sensitive X-Ray Scattering. In *Modern Characterization Methods of Surfactant Systems*; Binks, B. P., Ed.; Marcel Dekker, Inc: New York, 1999.
(46) Viney, C.; Russell, T. P.; Depero, L. E.; Twieg, R. J. *Mol. Cryst. Liq. Cryst.* **1989**, *168*, 63–82.

JP105114D